Preliminary Study of Flame Structure in an Internal Combustion Engine Using 2-D Flow Visualization

A.O. zur Loye and F.V. Bracco
Department of Mechanical and Aerospace Engineering, Princeton, New Jersey,
D.A. Santavicca
Department of Mechanical Engineering, Pennsylvania State University

ABSTRACT:

The structure of the turbulent flame in a premixed charge internal combustion engine was investigated at engine speeds of 300, 600, 1200, and 1800 rpm. A laser sheet, 200 microns thick and 1 cm wide, was passed through the turbulent flame front and the intensity of the light scattered by seeding particles was measured, thus obtaining two dimensional (2-D) cross-sections of the flame front. At the lower engine speeds the flame fronts were mostly continuous with some apparent pockets of unburned gas. As the engine speed was increased the flame fronts were more strongly distorted and the frequency of (what appeared to be) multiply connected flame sheets increased. The measured flame thicknesses varied from 300 microns to 1000 microns with the larger values more common at higher speeds. At least some of the variation was due to the flame being tilted with respect to the laser sheet but uncertainties persist as to the accuracy of the measured thicknesses.

INTRODUCTION

The interaction between the turbulent motion of the gases in internal combustion (I.C.) engines and the combustion process is essential for the operation of I.C. engines. Turbulence drastically increases the rate of combustion, as compared with that of a laminar flame. Moreover, the turbulence intensity increases almost linearly with engine speed [1,2] and thereby causes the rate of combustion to increase with engine speed. This allows engines to be run over a wide range of speeds. However, neither the turbulent flow field nor its effect on the structure of the flame are completely understood. At sufficiently low engine speeds (i.e. low turbulence intensities) the flame in an engine must resemble a slightly wrinkled laminar flame which propagates as a continuous sheet but it is not clear whether this model of an engine flame, which locally behaves as a one-dimensional quasi-steady laminar flame, is valid at engine speeds which are significantly higher than idle [3].

It is known from shadowgraph and schlieren photographs that the reaction zone in the engine is of the order of one cm thick [4,5], but because of the "line of sight integration" of these techniques no conclusions can be drawn about the actual structure of this zone. Recently, more sophisticated techniques have provided additional insight into the structure of turbulent flames in engines. Micro-schlieren photographs [6] of the flame front have indicated that the scale of the wrinkles in the flame front, as defined by the spacing of the lines on the schlieren pictures, decreases with increasing engine speed. One-dimensional Rayleigh scattering measurements [7] have shown that the likelihood of forming islands or peninsulas of unburned mixture increases with engine speed.

It is the objective of this study to improve our understanding of the structure of turbulent flames in I.C. engines by visualizing the shape of the flame front in two dimensions. The technique used differs significantly from shadowgraph and schlieren methods in that it produces a two dimensional image of a thin "slice" of the flame front, rather than an image which corresponds to an integration along the path of the light.

EXPERIMENT

The 2-D flow-visualization and engine set-up is shown schematically in figure 1. The measurements were taken in one of the transparent head engines in the Engine Combustion Laboratory at Princeton University. A schematic

drawing of the piston, cylinder and head assembly is shown in figure 2. This assembly was mounted on a high speed Waukesha CFR-48 crankcase and had an 8.26 cm bore and a 11.43 cm stroke. Intake and exhaust gases were passed through ports in the cylinder walls as in a two stroke engine. Extensive optical access was possible in this engine through windows mounted in the head and the cylinder. For this study a 10.16 cm diameter window was used in the head for the collection of the scattered light, and two 1.59 cm windows were located in the cylinder walls to allow the sheet of laser light to enter and exit the engine. The piston and head surfaces were flat so that the combustion chamber was pancake shaped with a compression ratio of 8 to 1 and a clearance height at top dead center (TDC) of 13 mm. The intake ports were directed 30 degrees from the cylinder radius to produce swirl and upward at 30 degrees to improve the scavenging efficiency. The timing of the exhaust and intake ports was +/- 113 degrees and +/- 126 degrees respectively, where 0 degrees is (TDC). Three bronze impregnated Teflon piston rings were used, enabling the engine to run without cylinder lubrication, thereby reducing the problem of window fouling.

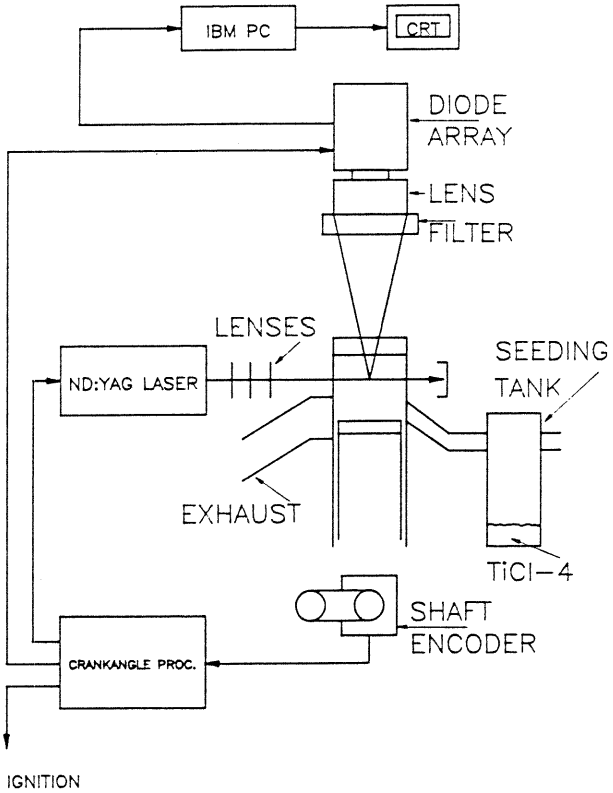

Fig. 1: 2-D Flow Visualization Experiment Schematic.

For the work presented in this paper the engine was run at 300, 600, 1200, and 1800 rpm. The swirl number at TDC was measured to be 4 at 1200 rpm and 3 at 1800 rpm [2]. The intake air was supplied by an air compressor at rates corresponding to 100 % volumetric efficiency. The intake manifold pressure was ambient (101.3 kPa) for 300 rpm and 600 rpm, and was equal to 108 kPa and 122 kPa for 1200 rpm and 1800 rpm respectively. The intake manifold temperature was 25 degrees C. The exhaust pressure was 99 kPa. For all the cases investigated, propane was used as the fuel at an equivalence ratio of 1.0. The spark timing was set at 15 degrees before TDC for all engine speeds. To ensure complete scavenging the engine was fired every fourth cycle when run at 300 and 600 rpm and every eighth cycle when run at 1200 and 1800 rpm.

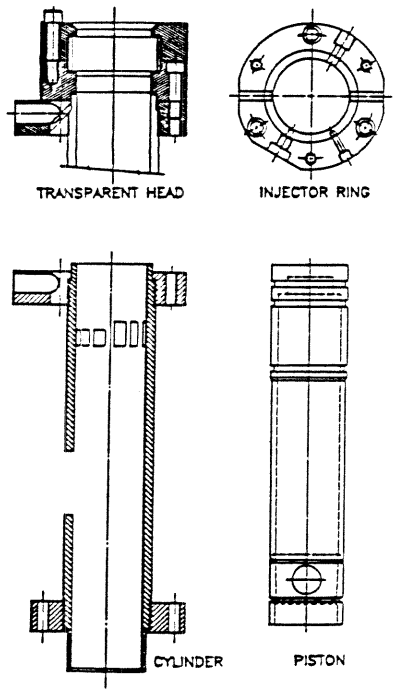

Fig. 2: Piston, Cylinder, and Cylinder Head Assembly.

The engine crankangle was monitored by an optical shaft encoder, the output of which was sent to a crankangle trigger module which was used to provide variable trigger pulses to control the timing of the ignition and laser pulse. In-cylinder pressure was measured with a water cooled piezoelectric transducer.

The laser was a Quanta Ray frequency doubled Nd:YAG with a 10 nano second pulse width. The laser was operated at approximately 200 millijoules per pulse. Using one plano-convex lens and two cylindrical lenses the laser beam was focused into a sheet which, at the measurement location, i.e. the center of the clearance volume, was less than 200 microns thick. The laser was pulsed when the flame front was near the center of the combustion chamber, about 5 degrees before TDC. The scattered light was first passed through a 10 nanometer halfwidth bandpass filter (full width at half height) with a center wavelength of 530 nanometers, and then focused onto a model MC521 reticon diode array by an F1.4 50 mm lens. To reduce flare the lens was stopped down to an F-number of 2.8. The diode array was unintensified and had a 100 x 100 pixel resolution. The magnification was adjusted to 1.7 which resulted in a field of view of 10 mm x 10 mm. Due to interfacing constraints, the actual images were made up of 98 x 96 pixels.

The signal from the diode array was digitized by a 12-bit Tecmar Labmaster A/D converter, then stored by an IBM PC, and displayed on a monitor in false color using a 16 color scale. The sampling rate of the A/D converter was 62.5 kHz which corresponded to 160 milliseconds per frame. Note, however, that the temporal resolution of the measurement, as determined by the pulse duration of the laser, was 10 nanoseconds (easily short enough to freeze the motion of the flame).

The intake air was seeded with titanium dioxide which was generated in a seeding chamber by reacting titanium tetrachloride vapor with the moisture in the intake air. This method, which has been used elsewhere [8-10], provided a uniform, high density distribution of sub-micron particles in the intake air. The effect of the seed on the combustion process itself was investigated by comparing pressure traces taken with and without seed. It was found to be negligible.

After the information from the diode array had been digitized the data was corrected for dark noise by subtracting a reference image obtained by taking an image while the laser sheet was blocked and the engine was not firing. The data was then corrected for systematic non-uniformities in pixel sensitivity, the laser sheet profile, and the collection optics. This last correction was achieved by normalizing the image by a second reference image which was the average of 10 frames taken under non-firing conditions minus the dark noise image. Each pixel in the corrected image was then assigned a color based on a linear scale which spanned all the intensity values in that particular image. This contrast enhancement technique automatically removed any noise pedestal. Due to the constraints imposed by the printer, the images shown in this paper are on a non-linear scale of three shades of gray, whereas during the analysis the images were viewed in 16 shades of blue, red and yellow. While some details are lost by using only three shades, the main features of the flame structure are still detectable.

The images thus obtained correspond to a two-dimensional density map, since the number density of the seed is proportional to the gas density. While this method is not capable of providing quantitative temperature information, it does clearly indicate the boundary between hot (burned) and cold (unburned) gases thus giving valuable information about the structure of the flame.

Before applying this visualization technique to turbulent flame fronts its capabilities were evaluated by determining the resolution of the system and by examining seeded jets. The resolution of the system was determined to be better than 200 microns. The resolution is slightly lower than the ideal resolution of one pixel (i.e. 100 microns) because of cross talk between the pixel elements on the array and flare in the collection optics.

The definition of the turbulence Reynolds number used in this work is $u'L/\nu$, where u' is the turbulence intensity, L is the integral length scale, and ν is the kinematic viscosity. The integral length scale was taken as (0.21)H, where H is the clearance height. This expression for the integral length scale was obtained by Launder and Spalding [11] using a boundary layer argument. Because of the lack of simultaneous multi-point velocity measurements in I.C. engines the accuracy of this expression is uncertain but is expected to be correct to within a factor of two. Earlier measurements of the turbulence intensity (u') in an identical engine [2], but run under motored conditions, were used. Since in [2] the engine had only been run at speeds above 1200 rpm, u' was assumed to be proportional to engine speed at lower rpm. The kinematic viscosity ν was taken to be 5.5 E-06 m**2/sec.

RESULTS

Figures 4(a) through 4(e) show "pictures" of the flame fronts at 300 rpm (u'=.75 m/s, Re=372), where the position of the single spark plug, the measurement location, and the direction of the swirl are indicated schematically in figure 3.

In figure 4 the white areas indicate low scattering intensity and therefore low density and high temperature, whereas the black areas represent high scattering intensity and therefore high density and low temperature. The gray areas show regions which correspond to the intermediate-density region of the flame front or to a section of the flame which only protrudes partially into the laser sheet from above or below. These pictures were chosen as typical for this particular engine speed. Examining figure 4 one can see that the flame fronts clearly resemble a gently wrinkled laminar flame. Each flame front consists of a continuous, singly connected sheet with the exception of the flame front in figure 4(a) where a small pocket of unburned gas can be seen.

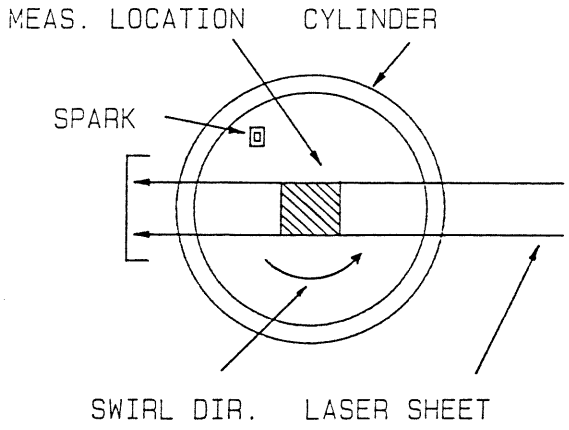

Fig. 3: Schematic of Measurement location and Swirl direction.

Figures 5(a) through 5(e) show results for 600 rpm (u'=1.5 m/s, Re=745). When comparing these pictures to the pictures taken at 300 rpm it becomes apparent that the increase in turbulence intensity has caused the flame fronts to become much more distorted and that the flame sheets more often appear to be multiply connected (islands of burned or unburned gas). However, given that the information contained in these images is two-dimensional, the possibility of a connection between the apparent islands and the main flame front in the third dimension cannot be ruled out. It is also apparent that the length of the flame front is larger than it was at 300 rpm.

Further increasing the engine speed to 1200 rpm (u'=3 m/s, Re=1489) results in severe distortion of the flame fronts, as can be seen in figures 6(a) through 6(e). In different cycles the character of the flame front changes from a structure that can be clearly identified as a distorted laminar flame (as was observed at the two lower engine speeds), to a structure that has a very different, "chopped" appearance. For the latter flames it becomes very difficult to imagine these flame fronts as consisting of single sheets somehow connected in the third dimension. The trend of increasing flame front length with larger engine speed can be seen when comparing these pictures to the ones taken at the lower engine speeds.

At 1800 rpm (u'=4.5 m/s, Re=2234), figures 7(a) through 7(e), the flame fronts resembled those at 1200 rpm with the difference that the "chopped" flame fronts became more frequent.

Figures 8(a) through 8(c) show individual horizontal cross-sections taken from images obtained at 300 rpm in places where the flame front was vertical in the plane of the picture. The locations of these cross-sections are marked with arrows in figure 4 (the top arrow in figure 4 corresponds to the top cross-section in figure 8 and so forth).

From examining many such cross-sections it was determined that the measured flame thickness varied approximately from 300 microns to 800 microns. At least a fraction of this variation in measured flame thickness is due to a tilt of the flame front relative to the measurement plane. The actual flame thickness would then be equal to the smallest measured flame thickness i.e. 300 microns, corresponding to the situation where the flame front is near normal to the measurement plane. However, it should be noted that the validity of this technique for determining the flame thickness has not been established. Indeed, on the one hand it is possible that the flame thickness thus deduced is smaller than in reality due to a drastic decrease in scattering cross-section of the particles across the flame. On the other hand, the 200 micron resolution of the system may cause the measured flame to be thicker than is actually the case.

Figures 9(a) through 9(c) show several cross-sections of the pictures taken at 600 rpm. Examination of many such cross-sections showed that the range of the measured flame thicknesses is slightly larger than the range observed at 300 rpm, about 300 microns to 1000 microns, and that larger measured flame thicknesses became more frequent. At least in part this is due to the higher degree of convolution of the flame fronts, which can also be expected to be present in the planes normal to the measurement plane. More convoluted flame fronts imply that the front is less likely to be perpendicular to the measurement plane.

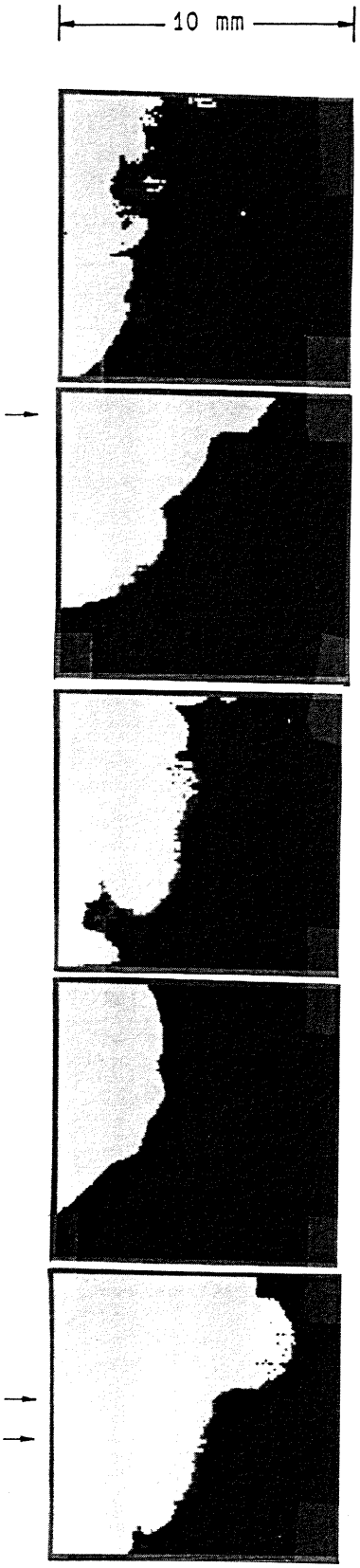

Fig. 4: (a - e): Images of Turbulent Flame Fronts Taken at 300 RPM.

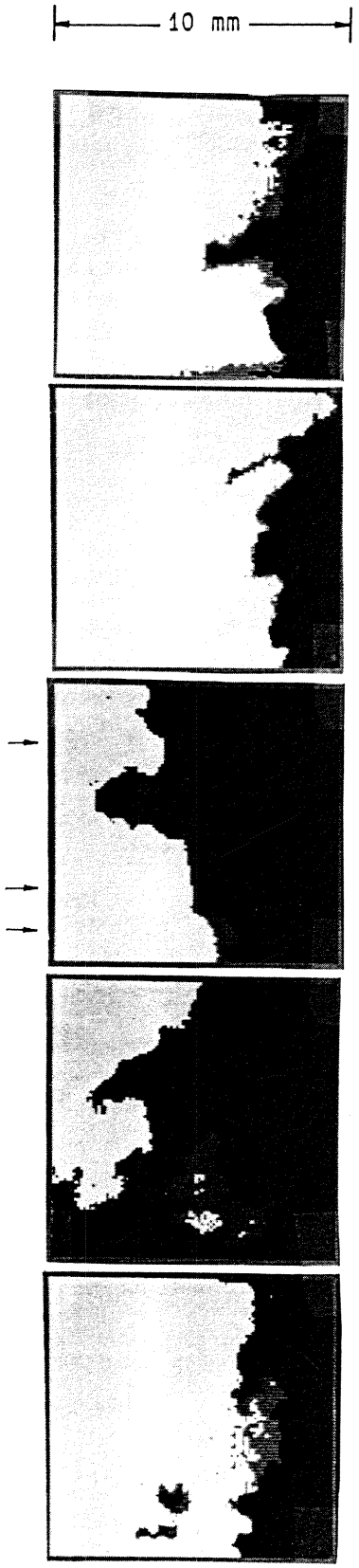

Fig. 5: (a - e): Images of Turbulent Flame Fronts Taken at 600 RPM.

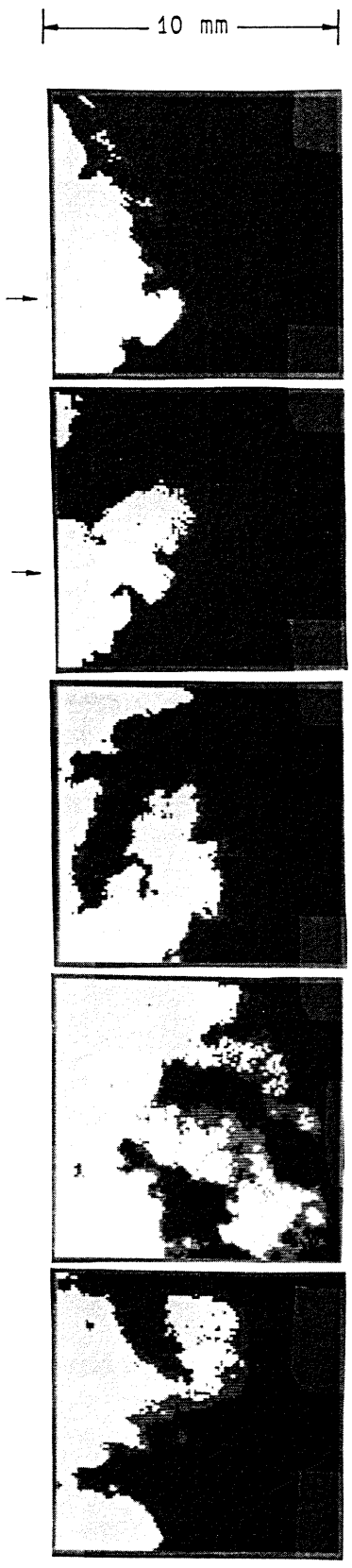

Fig. 6: (a - e): Images of Turbulent Flame Fronts Taken at 1200 RPM.

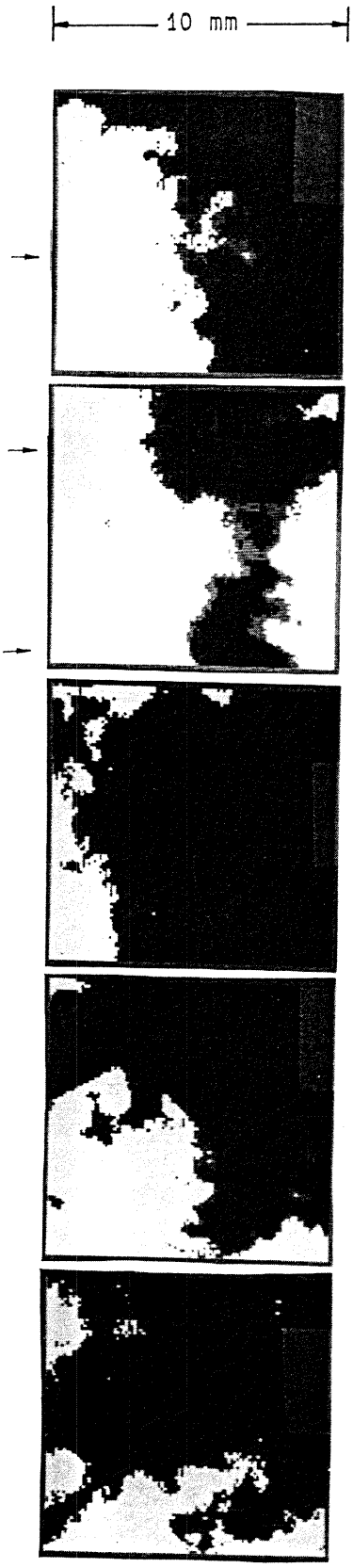

Fig. 7: (a - e): Images of Turbulent Flame Fronts Taken at 1800 RPM.

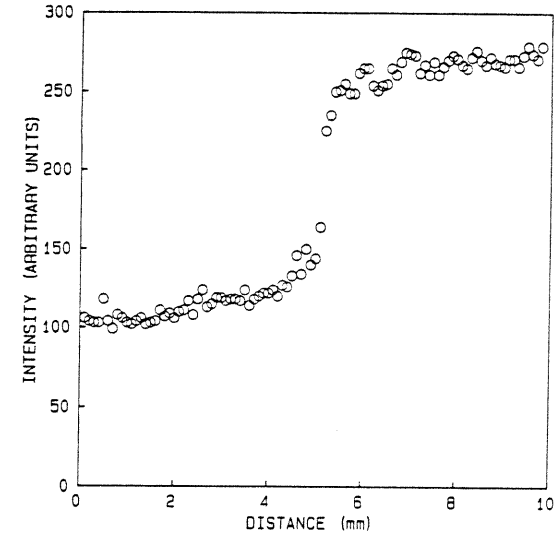

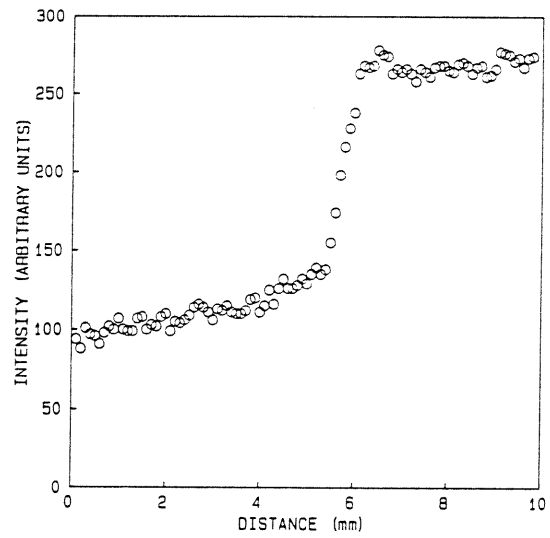

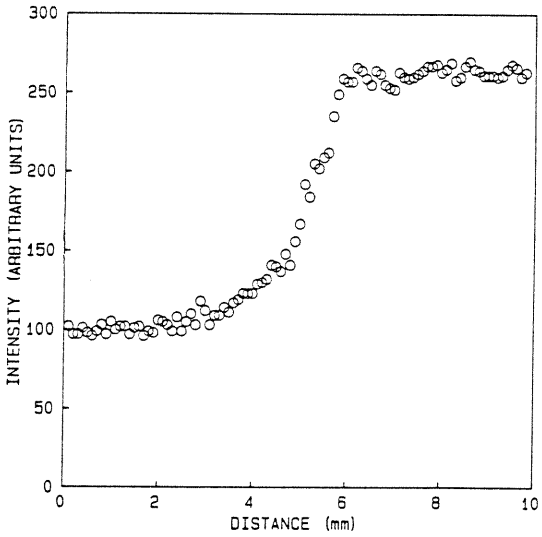

Fig. 8: (a,b,c): 1-D Cross-sections From Images Taken at 300 RPM.

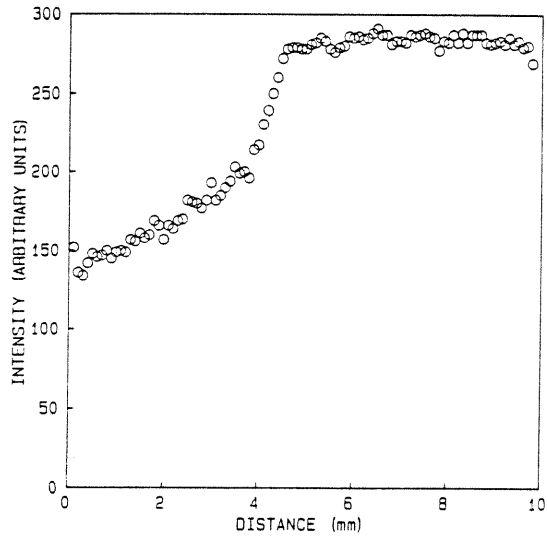

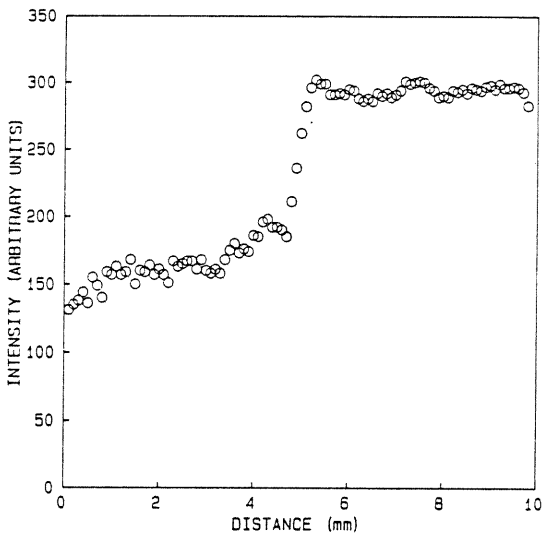

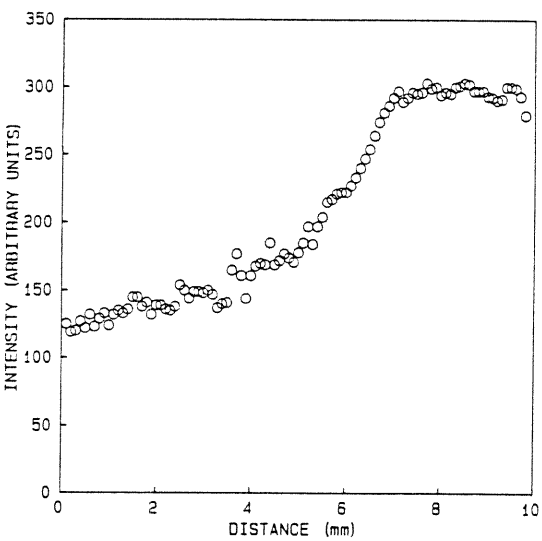

Fig. 9: (a,b,c): 1-D Cross-sections From Images Taken at 600 RPM.

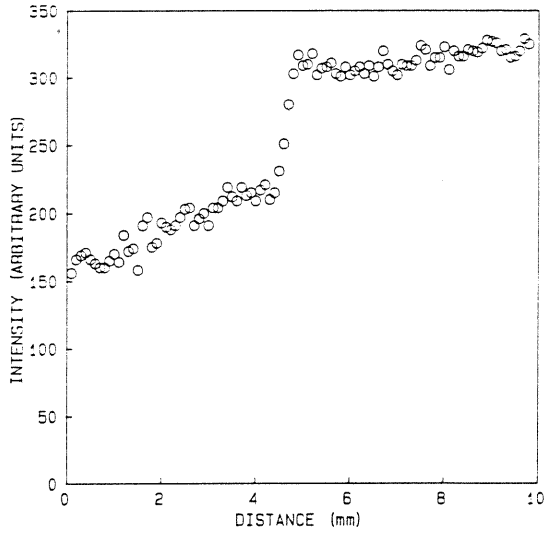

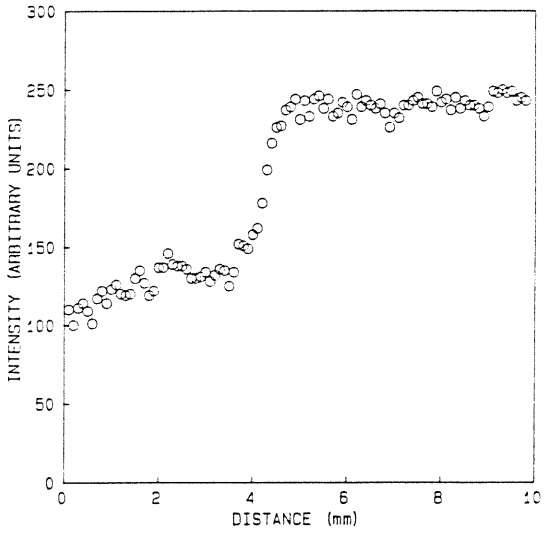

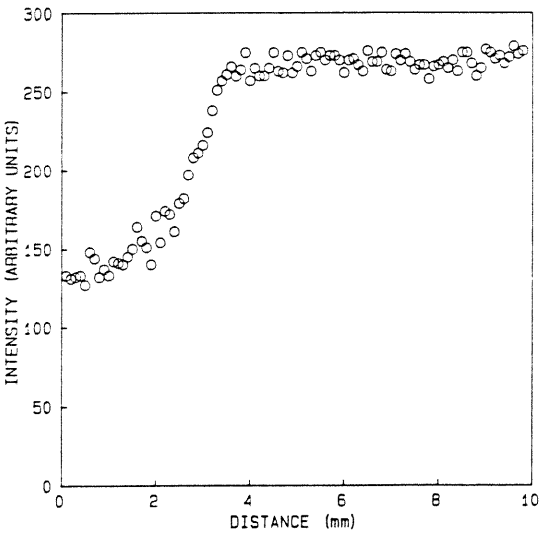

Fig. 10: (a,b,c): 1-D Cross-sections From Images Taken at 1200 RPM.

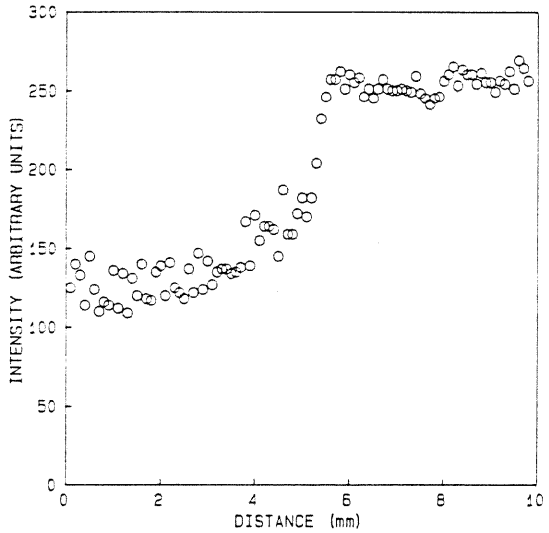

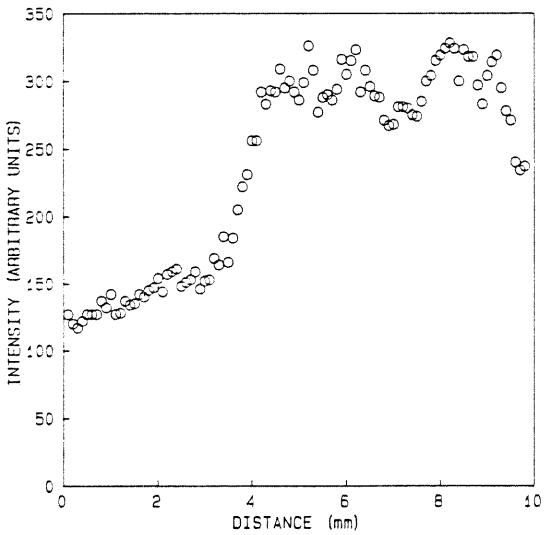

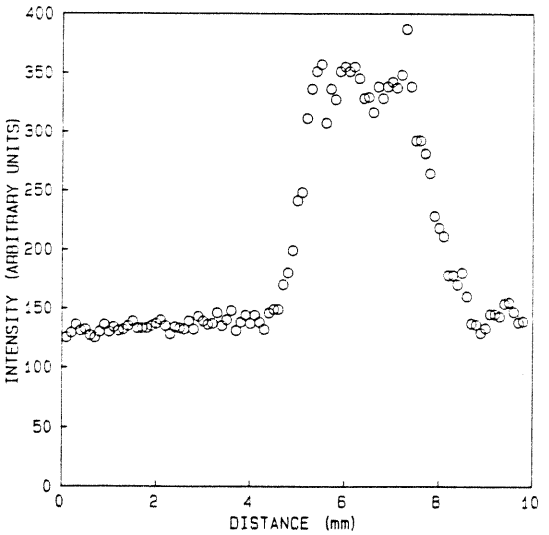

Fig. 11: (a,b,c): 1-D Cross-sections From Images Taken at 1800 RPM.

Figures 10(a) through 10(c) show cross-sections taken from pictures obtained at 1200 rpm. The range of measured flame thicknesses, about 300 microns to 1000 microns, is roughly the same as that observed at 600 rpm. The frequency of the larger measured flame thicknesses continues to increase. This trend is paralleled by more distorted flame fronts, which implies that the apparent thickening of the flames can be due to an increased probability of flame fronts occurring at angles very different from 90 degrees relative to the measurement plane.

Cross-sections of the pictures taken at 1800 rpm are shown in figures 11(a) through 11(c). These cross-sections are similar to those obtained at 1200 rpm in that the range of measured flame thicknesses was roughly the same as that observed at 1200 rpm and the most probable measured flame thickness was larger than that at observed at 300 and 600 rpm.

This trend of increasing mean measured flame thickness with engine speed was also observed by Smith [7]. Smith reported a minimum flame thickness of about 100 microns at engine speeds ranging from 300 to 1800 rpm, using stoichiometric methane air mixtures, which is less than the 300 microns observed in this experiment. This difference is probably due to the different fuels and to the limited resolution of the camera used in this experiment.

For the cases investigated in this experiment, the flame fronts are found to become more wrinkled as engine speed is raised. This conclusions agrees with the findings of Smith's micro-schlieren study [6] and his one-dimensional Rayleigh scattering experiment [7].

CONCLUSIONS

A two-dimensional visualization technique based on Mie scattering by titanium dioxide particles and illumination by a sheet of pulsed laser light was applied to study the flame structure in an I.C. engine at speeds ranging from 300 rpm to 1800 rpm. By studying the images obtained using this technique the following conclusions are drawn about the structure of the turbulent flame:

1) At low engine speeds (300 rpm and 600 rpm), mostly continuous flame fronts with slight wrinkling are observed. Apparent pockets of unburned gas are observed at both 300 and 600 rpm and are more frequent at 600 rpm.

2) At higher engine speeds (1200 rpm and 1800 rpm), the flame front is severely distorted and the frequency of (what appeared to be) multiply connected flame sheets is higher than at lower speeds.

3) The measured flame thicknesses at 300 rpm varies from about 300 microns to 800 microns. At 600, 1200 and 1800 rpm it varies from as little as 300 microns to about 1000 microns and greater thicknesses occur more frequently at the higher speeds.

4) The variation of measured flame thickness at constant engine speed is, at least in part, due to the the flame front not being perpendicular to the measurement plane, while the increase of measured flame thickness with increasing engine speed probably results from the higher degree of distortion of the flame front. This distortion decreases the probability of the front being perpendicular to the laser sheet. However uncertainties persist about the accuracy of the measured flame thicknesses.

ACKNOWLEDGEMENTS

The authors would like to thank Mr. J. Semler for his technical support and G. Russell and T. Lee for their help in developing the data acquisition software. Support for this work was provided by the Department of Energy (contract DE-AC-04-81-AL16338), General Motors, and Cummins Engine. Some of the results were presented at the 21st DISC meeting, Washington, DC, March 1985.

REFERENCES

1. Lancaster, D.R., "Effects of Engine Variables on Turbulence in a Spark Ignition Engine", SAE Paper 760159, 1976.

2. Liou, T.M., Hall, M., Santavicca D.A., and Bracco, F.V. "Laser Doppler Velocimetry Measurements in Valved and Ported Engines", SAE Paper 840375, 1984.

3. Abraham, J., Williams, F.A., and Bracco, F.V. "A Discussion of Turbulent Flame Structure in Premixed Charges", SAE Paper 850345, 1985.

4. Witze, P.O., "An Optical Imaging Technique for Measuring Time Resolved Flame Position", Fall Meeting of the Western States Section of the Combustion Institute, Paper WSS/CI 84-71, 1984.

5. Namazian, M., Hansen, S., Lyford-Pyke, E., Sanchez-Barsse, J., Heywood, J., and Rife, J., "Schlieren

Visualization of the Flow and Density Fields in the Cylinder of a Spark-Ignition Engine," SAE Paper 800044, 1980.

6. Smith, J.R., "The Influence of Turbulence on Flame Structure in an Engine", Sandia Report SAND82-8722, 1982

7. Smith, J.R., "Turbulent Flame Structure in a Homogeneous-Charge Engine", SAE Paper 820043, 1982.

8. Cozzi, C., and Cadorin, D., "Nucleation, Growth and Coagulation of Solid Particles in Flames", Combustion Science and Technology, Vol 5, pp. 213-218, 1972.

9. Ebrahimi, I., and Kleine, R., "The Nozzle Fluid Concentration Field in Round Turbulent Free Jets and Jet Diffusion Flames", Sixteenth International Symposium on Combustion, p. 1711, the Combustion Institute, 1977.

10. Moss, J.B., "Simultaneous Measurements of Concentration and Velocity in an Open Premixed Flame", Combustion Science and Technology, Vol 22, pp. 119-129, 1980.

11. Launder, B.E. and Spalding, D.B., Lectures in Mathematical Models of Turbulence, Academic Press, p. 79, 1972.